

Vortex Avalanches and Magnetic Flux Fragmentation in Superconductors

Igor Aranson,¹ Alex Gurevich,² and Valerii Vinokur¹

¹Materials Science Division, Argonne National Laboratory, Argonne, Illinois 60439

²Applied Superconductivity Center, University of Wisconsin, Madison, Wisconsin 53706

(Received 17 April 2001; published 20 July 2001)

We report the results of numerical simulations of nonisothermal dendritic flux penetration in type-II superconductors. We propose a generic mechanism of dynamic branching of a propagating hot spot of a flux flow/normal state triggered by a local heat pulse. The branching occurs when the flux hot spot reflects from inhomogeneities or the boundary on which magnetization currents either vanish, or change direction. The hot spot then undergoes a cascade of successive splittings, giving rise to a dissipative dendritic-type flux structure. This dynamic state eventually cools down, turning into a frozen multifilamentary pattern of magnetization currents.

DOI: 10.1103/PhysRevLett.87.067003

PACS numbers: 74.60.Ge, 74.20.De, 74.25.Ha

The formation of a macroscopic current-carrying critical state in type-II superconductors occurs via penetration of the magnetic flux front of pinned vortices from the surface of the sample. This process is controlled by a highly nonlinear electric field-current density (E - J) characteristics $E(J, T, B)$, which together with the Maxwell equations determine macroscopic electrodynamics of superconductors [1–3]. Propagating magnetic flux causes joule heating, giving rise to global flux jumps and thermal quench instabilities which are crucial for stable operation of current-carrying superconductors [4,5]. The magneto-optical imaging has revealed a new class of instabilities of the critical state, including magnetic macroturbulence [6,7], kinetic front roughening [8], magnetic avalanches [9], and dynamic dendritic structures [10–12]. The latter have been observed both on high- T_c ($\text{YBa}_2\text{Cu}_3\text{O}_7$ [10]) and on low- T_c (Nb [11]), superconducting films, and most recently on the newly discovered MgB_2 [12]. These instabilities are rather characteristic of superconductors; besides they also display remarkable similarities with other dendritic instabilities in crystal growth [13], nonequilibrium chemical and biological systems [14], and crack propagation [15].

We performed numerical simulations of coupled equations for the magnetic induction $B(\mathbf{r}, t)$ and temperature $T(\mathbf{r}, t)$ and found a new mechanism of flux fragmentation in superconductors, which is different from the well-known bending instability of moving interface between two phases [13], and results from the generic distribution of magnetization currents in the critical state. Our results give insight into vortex microavalanches and flux jumps in superconductors.

We focus on a slab in a magnetic field B_0 (Fig. 1), for which distributions of the z component of magnetic induction, $B(\mathbf{r}, t)$, and temperature, $T(\mathbf{r}, t)$, are described by the Maxwell equation coupled to the heat diffusion:

$$C \partial_t T = \text{div} \kappa \nabla T - h(T - T_0)/d + JE(J, T), \quad (1)$$

$$\partial_t B = -c \nabla \times \mathbf{E}(J, T), \quad \mathbf{J} = (c/4\pi) \hat{z} \times \nabla B. \quad (2)$$

Here $C(T)$ is the heat capacity, $\kappa(T)$ is the thermal conductivity, $h(T)$ is the heat transfer coefficient to the coolant held at the temperature T_0 , $d = A/P$, A is the area of the sample cross section, P is the perimeter of the cooled sample surface, and $E(J, T)$ is the modulus of the electric field, which essentially depends on both the local temperature $T(\mathbf{r}, t)$ and the current density, $J(\mathbf{r}, t) = (J_x^2 + J_y^2)^{1/2}$. The spatial derivatives are taken

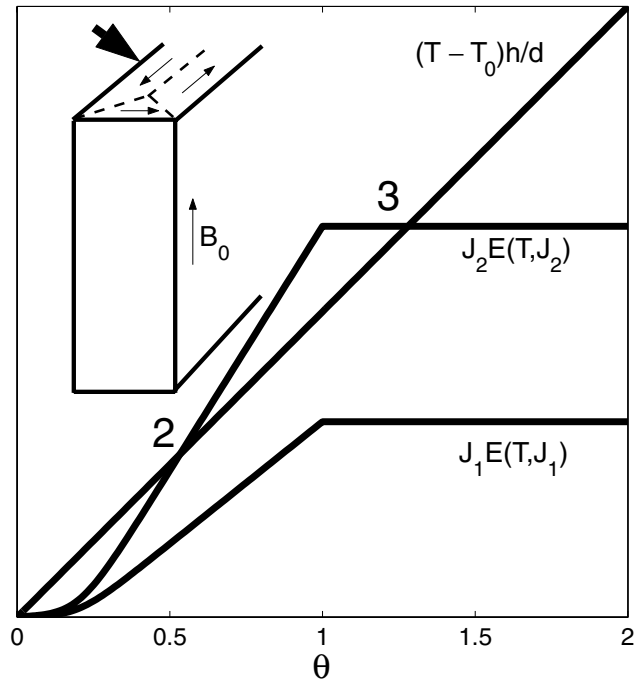


FIG. 1. Graphic solution of the heat balance condition $(T - T_0)h/d = JE(\theta, J)$ in a superconductor. The power of the joule heat release $JE(J, \theta)$ is plotted as a function of T for $J_1 < J_m$ and $J_2 > J_m$, where $E(J, \theta)$ is given by Eq. (3), and $\theta = (T - T_0)/(T^* - T_0)$. The inset shows the sample geometry, the magnetic field is parallel to the z axis, the x axis is directed along the sample surface, and y is perpendicular to the sample surface. The local heat pulse (indicated as the large arrow) triggers the magnetic hot spot propagation across magnetization currents presented in detail in Figs. 2 and 3.

with respect to x and y , while the term $h(T - T_0)/d$ accounts for the surface cooling [16]. We will consider the case of high magnetic fields B_0 , much greater than the field of full magnetic flux penetration, $B_p \sim 4\pi J_c d/c$, for which $E(J, T, B) \approx E(J, T, B_0)$.

The evolution of $T(\mathbf{r}, t)$ and $B(\mathbf{r}, t)$ is mostly determined by the $E(T, J)$ characteristic, which accounts for the high-resistive flux flow state at $J > J_c$ and the low-resistive flux creep state at $J < J_c$, where J_c is the critical current density. The effects considered in this paper are not very sensitive to the details of $E(J, T)$, so for the numerical simulations of Eqs. (1) and (2) we take the following interpolation formula expressed in terms of observable parameters J_c , J_1 , and ρ :

$$E = \rho J_1 \ln[1 + \exp(J - J_c)/J_1]. \quad (3)$$

Here $J_1(T) = \partial J / \partial \ln T$ is the dynamic flux creep rate, and $\rho(T) = \rho_n B / B_{c2}$ is the flux flow resistivity. Below the irreversibility field $B < B^*$, where $J_1 \ll J_c$, Eq. (3) reproduces the main features of $E(J, T)$ observed in experiment, giving a linear flux flow dependence $E = (J - J_c)\rho$ for $J > J_c$ and the exponential dependence $E = E_c \exp(J - J_c)/J_1$ for $J < J_c$.

The similarity of Eqs. (1) and (2) with generic reaction-diffusion equations [14] is due to the thermal bistability of superconductors [5], for which the heat balance condition $(T - T_0)h/d = JE(T, J)$ in the right-hand side of Eq. (1) is satisfied for three different temperatures T , as shown in Fig. 1. Here the points 0 and 3 correspond to two stable uniform states: a cold superconducting state with $T \approx T_0$ and a hot flux flow/normal state T_3 self-sustained by joule heating. As seen from Fig. 1, the bistability occurs if the current density J exceeds a threshold value J_m , for which $\rho J_m^2 \approx h(T^* - T_0)/d$. Hence, $J_m \approx [(T^* - T_0)h/d\rho]^{1/2}$, where $T^*(B)$ is the irreversibility temperature at which $J_c(T^*) = 0$. The superconducting state is unstable with respect to the hot spot formation, if $\alpha_s = (J_c/J_m)^2 > 1$. For typical parameters of HTS films at $T_0 = 4.2$ K ($\rho \sim 100 \mu\Omega$ cm, $J_c = 10^6$ – 10^7 A/cm², $h \sim 1$ W/cm² K, $T^* - T_0 \sim 50$ – 100 K, and $d = 1 \mu$ m), we obtain $\alpha_s \sim 10^2$ – 10^4 , thus the thermal bistability is a characteristic feature of both high temperature (HTS) and low temperature (LTS) superconductors, especially films because of their higher J_c values [5].

We consider the case of weak joule heating, $T(x, y, t) \approx T_c$, for which we take into account only the most essential temperature dependence of $E(T)$, while $C(T)$, $h(T)$, and $\kappa(T)$ can be taken at $T = T_0$. Then Eqs. (1) and (2) can be written in the following dimensionless form:

$$\tau \dot{b} = \partial_x[r(j, \theta)\partial_x b] + \partial_y[r(j, \theta)\partial_y b], \quad (4)$$

$$\dot{\theta} = \nabla^2 \theta - \theta + \alpha j^2 r(j, \theta). \quad (5)$$

Here $\theta = (T - T_0)/(T^* - T_0)$, $b = B/B_t$, and $j = [(\partial_x b)^2 + (\partial_y b)^2]^{1/2}$ are the dimensionless temperature, magnetic field, and current density, respectively, and

$B_t = 4\pi J_1 L_h / c$. The derivatives in Eqs. (4) and (5) are taken with respect to normalized time t/t_h and coordinates x/L_h and y/L_h measured in the thermal units $t_h = Cd/h$ and $L_h = (d\kappa/h)^{1/2}$. The evolution of $\theta(\mathbf{r}, t)$ and $b(\mathbf{r}, t)$ is controlled by two dimensionless parameters:

$$\tau = \frac{4\pi\kappa}{\rho C c^2}, \quad \alpha = \frac{\rho J_1^2 d}{h(T^* - T_0)}. \quad (6)$$

Here τ is the ratio of the diffusivities of heat and magnetic flux, and α quantifies joule dissipation. For Nb films of Ref. [11], we obtain $\tau \sim 10$ at 4.2 K, with τ rapidly decreasing with increasing T_0 . For HTS at 77 K, we obtain $\tau \sim 10^{-4}$ – $10^{-5} \ll 1$. The nonlinear resistivity $r(j, \theta) = \ln[1 + \exp(j - j_c(\theta))]/j$ obtained from Eq. (3) has asymptotics $r = 1 - j_c/j$ in the flux flow ($j > j_c$) and $r = \exp(j - j_c)/j$ in the flux creep ($j < j_c$) states, where $j_c = J_c(T)/J_1$. We linearize $j_c = j_0(1 - \theta)$ around T_0 , neglecting the temperature dependencies of J_1 , ρ [17].

We performed 2D numerical simulations of Eqs. (4) and (5) to calculate propagation of a magnetic hot spot of resistive phase across a superconductor (see Fig. 1). The process is initiated by a local heat pulse applied to the sample surface, which models the experiment by Leiderer *et al.* [10], who triggered the magnetic dendrite instability by a laser pulse. To address the effect of material inhomogeneities, we considered both uniform superconductors with J_c independent of spatial coordinates and nonuniform superconductors with the critical current density periodically modulated over macroscopic scales $2\pi/k$, much larger than the spacing between flux lines, $J_c(x, y, T) = J_{c0}(T)[1 + \epsilon \sin(kx) \sin(ky)]$ with $\epsilon < 1$. The latter case also models superconducting films with periodic arrays of holes, which have recently attracted much interest [18,19]. The resulting evolutions of the temperature distributions shown in Figs. 2 and 3 display a rather striking behavior which is described below.

For $\tau \ll 1$, the heat pulse applied to a uniform superconductor triggers a hot spot propagation across the sample, as shown in Fig. 2a. Such propagation appears stable until the hot domain reaches the center of the sample, where magnetization currents change direction. The resistive domain then undergoes a cascade of successive splittings into alternating stripes of low and high electric fields and temperatures. After each splitting, the part of the resistive domain near the central line cools down, but then the hot filaments of the resistive state start propagating again from the upper part of the resistive domain through the preceding dendritic structure toward the central line. However, each time the hot filaments cross the central line, they split again, causing new dendrites of alternating low and high J filaments to grow, as shown in Figs. 2b and 2c. Eventually the joule dissipation causes the electric field in the hot dendritic structures to decay below the threshold, thus a frozen entangled pattern of current filaments forms.

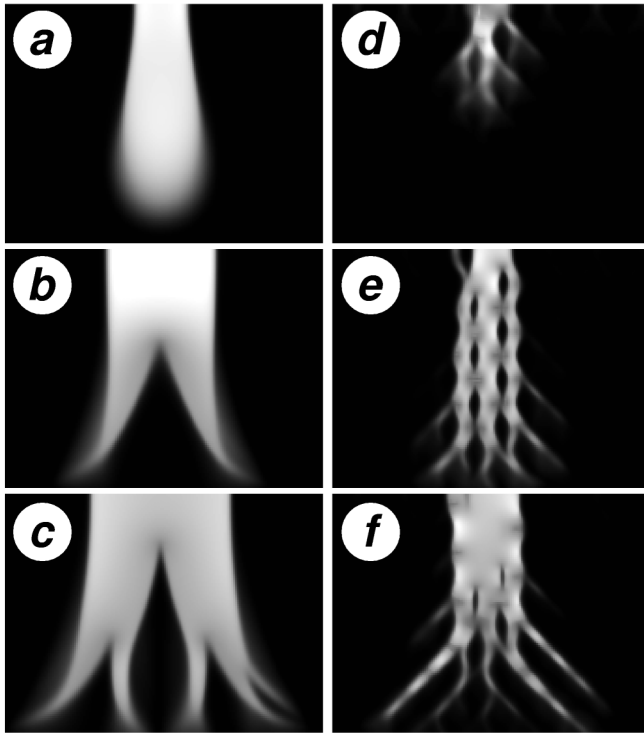


FIG. 2. Gray-coded dynamic temperature maps $\theta(\mathbf{r}, t)$ for the flux fragmentation instability in the homogeneous system for $t/t_h = 8$ (a), 20 (b), and 34 (c) at $\alpha = 0.008$, $\tau^{-1} = 150$, and the initial current in the Bean state, $j_0 = 18$ (white corresponds to $\theta > 1$, and black corresponds to $\theta = 0$). Domain of integration: $-150L_h < y < 150L_h$, $0 < x < 600L_h$, periodic boundary conditions in the x direction; no-flux $\partial\theta/\partial y$ at $y = \pm 150L_h$ for the temperature and $b = \text{const}$ for the magnetic field. Each panel shows the upper half of the sample and one-third of the total length: $0 < y < 150L_h$, $200L_h < x < 400L_h$. The magnetization currents change direction on the bottom part of each panel, i.e., for $y = 0$. Same for the system with periodic modulation in $J_c(x, y)$ for $2\pi/k = 30L_h$, $\epsilon = 0.5$, $t = 6$ (d), 16 (e), 28 (f), and $j_0 = 20$.

As follows from Figs. 2d–2f, spatial inhomogeneities in J_c can bring about new features of the hot spot propagation. The periodic modulation of $J_c(x, y)$ also gives rise to additional side branching and preferential flux propagation along the nearest neighbor directions at angles $\pm 45^\circ$, causing further interconnection of neighboring hot spot branches. This effect is similar to that observed in superconducting films with periodic arrays of holes and magnetic dots [19]. For $\tau \ll 1$, the diffusion of magnetic flux in the normal state occurs much faster than the heat diffusion. Therefore, magnetic flux rapidly penetrates the hot regions of the filamentary current structure in Fig. 2, forming dendritic flux front patterns reminiscent of those observed in magneto-optical experiments [10–12].

The flux fragmentation can be described as follows. For $\tau \ll 1$, the electric field \mathbf{E} becomes nearly potential, $\nabla \times \mathbf{E} \approx \mathbf{0}$, thus the magnetization currents tend to bypass the propagating hot resistive domain [20]. Thus, the current density in the resistive domain decreases, forcing

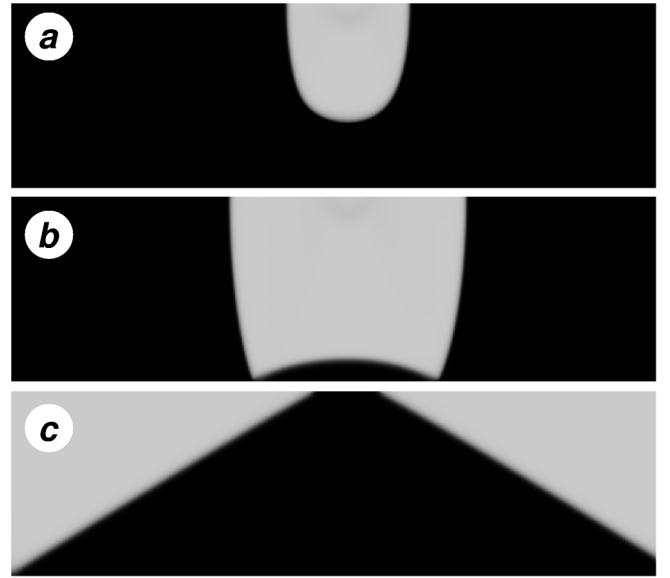


FIG. 3. Same dynamic temperature maps as in Fig. 2 for $\tau = 1$, $\alpha = 0.006$, $j_0 = 18$, and $t/t_h = 8$ (a), 20 (b), 34 (c).

the excess magnetization currents to flow along the domain interface. The high interface currents cause strong local enhancement of electric field and dissipation, widening the resistive domain near its end and accelerating the propagation velocity. At the same time, the temperature in the center of the resistive domain decreases, facilitating recovery of the superconducting state when the domain crosses the central line, where magnetization currents change direction. In this region the interface currents at the bottom part of the domain are partly compensated by the opposite magnetization currents, which strongly reduce joule dissipation and stops hot spot propagation. As a result, a triangular region at the tip of the resistive domain becomes superconducting, and then the process repeats as described above.

For $\tau \gg 1$, the hot spot propagation occurs at the frozen distribution of magnetic fields and currents, and the dynamics changes (as shown in Fig. 3). The heat pulse first initiates stable propagation of a resistive hot spot, then it splits into two parts which move apart and eventually disappear. This behavior occurs if the energy of the heat pulse Q is below the critical value Q_c . For $Q > Q_c$, the heat pulse creates a larger hot spot which then expands and propagates over the entire sample [5].

The dendritic flux penetration can be regarded as a *microavalanche* of a large bundle of vortices, which does not trigger a global flux jump instability or thermal quench of the whole sample. Such microavalanches cause only local transient temperature spikes, leaving behind the frozen flux dendrite structures shown in Fig. 4. Each avalanche thus results in a partial flux penetration, which reduces the total magnetic moment of a sample and manifests itself in steps on magnetization curves $M(B)$. Notice that microavalanches in increasing magnetic field may also

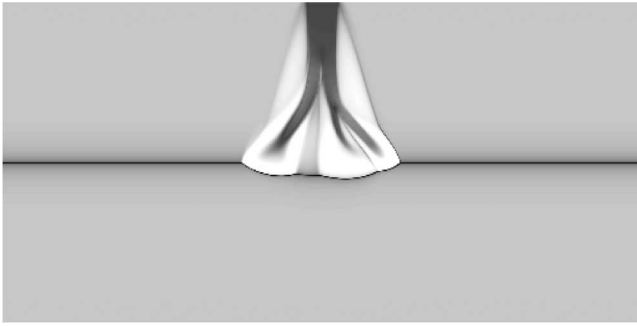


FIG. 4. A typical “frozen” current configuration after completion of the fragmentation for $\tau^{-1} = 600$. The gray shades change from black ($J = 0$) to white (maximum J). Full domain of integration is shown. The black line in the middle is due to reverse of direction of the magnetization current.

be initiated by surface defects (regions with lower J_c), which are sources of excess steady-state joule dissipation. Such common defects, which have been revealed by magneto-optical imaging of HTS [21], can trigger both global flux jumps [4] and local vortex microavalanches. The microavalanches cause steps in $M(B)$, as observed on Nb films at low temperatures [9]. After many microavalanches, the critical state eventually turns into a frozen “turbulent” current structure built of individual dendritic fragments, like that in Fig. 4.

The results of this work may capture the essential physics of dendritic flux instability observed on $\text{YBa}_2\text{Cu}_3\text{O}_7$ [10], Nb [11], and MgB_2 [12] films, although, for a more quantitative comparison, other factors should also be taken into account. The experiments [10–12] correspond to thin films in low perpendicular magnetic fields, which require the account of the nonlocal flux diffusion [3] and the geometrical barrier [22], whereas our model describes a slab in high parallel magnetic fields. Another intriguing result discovered in Ref. [10] is a superfast flux propagation with the velocities exceeding the speed of sound c_s . This also requires invoking additional mechanisms, because the thermal velocities of hot spot propagation $v \sim J[\kappa\rho/(T^* - T_0)]^{1/2}/C$ [5] is smaller than c_s . The superfast flux propagation might be due to electron overheating, so that an equation similar to Eq. (1) actually describes the electron temperature, higher than the lattice temperature T_0 . The lattice heat capacity C in the above estimate for $v(J)$ is then replaced by a much smaller electron heat capacity, which increases $v(J)$ by 1–2 orders of magnitude. This situation may occur at low T , if the time of the electron-phonon energy relaxation becomes larger than the thermal time t_h [23].

We proposed a new mechanism of magnetic flux fragmentation in superconductors. The instability manifests itself as a vortex microavalanche, accompanied by a transient local joule dissipation and eventually results in a frozen multifilamentary structure of magnetization currents. These effects give rise to dendritic flux penetration

into superconductors, partial flux jumps, and steps on magnetization curves.

This work was supported by the NSF MRSEC (DMR 9214707) (A. G.), U.S. Department of Energy, BES-Materials Sciences (W-31-109-ENG-38) (I. A. and V. V.). We are grateful to Peter Kes and Wim van Saarloos for hospitality during the initial stage of this work and to Vitalii Vlasko-Vlasov for illuminating discussions.

- [1] M. R. Beasley, R. Labusch, and W. W. Webb, *Phys. Rev.* **181**, 682 (1969); Y. Yeshurun, A. P. Malozemoff, and A. Shaulov, *Rev. Mod. Phys.* **68**, 911 (1996).
- [2] G. Blatter *et al.*, *Rev. Mod. Phys.* **66**, 1125 (1994).
- [3] E. H. Brandt, *Rep. Prog. Phys.* **58**, 1465 (1995).
- [4] R. G. Mints and A. L. Rakhmanov, *Rev. Mod. Phys.* **53**, 551 (1981).
- [5] W. J. Skocpol, M. R. Beasley, and M. Tinkham, *J. Appl. Phys.* **45**, 4054 (1974); A. V. Gurevich and R. G. Mints, *Rev. Mod. Phys.* **59**, 941 (1987).
- [6] V. K. Vlasko-Vlasov *et al.*, *Physica (Amsterdam)* **222C**, 361 (1994).
- [7] M. R. Koblishka *et al.*, *Europhys. Lett.* **41**, 419 (1998).
- [8] R. Surdeanu *et al.*, *Phys. Rev. Lett.* **83**, 2054 (1999).
- [9] E. R. Nowak *et al.*, *Phys. Rev. B* **55**, 11 702 (1997).
- [10] P. Leiderer *et al.*, *Phys. Rev. Lett.* **71**, 2646 (1993); U. Bolz *et al.*, *Physica (Amsterdam)* **284B–288B**, 757 (2000).
- [11] C. A. Duran *et al.*, *Phys. Rev. B* **52**, 75 (1995).
- [12] T. H. Johansen *et al.*, *cond-mat/0104113*.
- [13] D. A. Kessler, J. Koplik, and H. Levine, *Adv. Phys.* **37**, 255 (1988).
- [14] E. Ben-Jacob, I. Cohen, and H. Levine, *Adv. Phys.* **49**, 395 (2000).
- [15] I. S. Aranson, V. A. Kalatsky, and V. M. Vinokur, *Phys. Rev. Lett.* **85**, 118 (2000).
- [16] The term $h(T - T_0)/d$ accounts for the heat removal from a slab in a parallel field, for which this term provides the correct integral heat balance, $(T - T_0)h/d = JE(T)$, if we adopt the effective boundary conditions, $\partial_y T = 0$, at the surface. Our qualitative results are not sensitive to the thermal boundary conditions, because the dendritic flux instability occurs in a central region of the sample, and the velocity of the hot spot propagation for $\alpha_s \gg 1$ is independent of h [5].
- [17] The temperature independent J_1 is characteristic of low- T_c superconductors, where J_1 is mostly determined by local inhomogeneities of pinning [see, e.g., A. M. Campbell and J. E. Evetts, *Adv. Phys.* **21**, 1191 (1972)].
- [18] V. V. Moshchalkov *et al.*, *Phys. Rev. B* **57**, 3615 (1998).
- [19] V. K. Vlasko-Vlasov *et al.*, *Physica (Amsterdam)* **341C–348C**, 1281 (2000).
- [20] A. Gurevich and J. McDonald, *Phys. Rev. Lett.* **81**, 2546 (1998).
- [21] A. E. Pashitskii *et al.*, *Science* **275**, 367 (1997).
- [22] E. H. Brandt and M. V. Indenbom, *Phys. Rev. B* **48**, 12 893 (1994); E. Zeldov *et al.*, *Phys. Rev. Lett.* **73**, 1428 (1994).
- [23] A. Rothwarf and B. N. Taylor, *Phys. Rev. Lett.* **19**, 27 (1967).